ELECTRICAL ENGINEERING

IoT-Based Supervisory Control and Data Acquisition for Solar Microgrid Operation in Bonny Island

Richard Zarapege, H. N. Amadi

Department of Electrical Engineering, Faculty of Engineering, Rivers State University, Port Harcourt, Nigeria

Published November 2026

Abstract

An IoT-enabled SCADA system was designed and tested for real-time supervisory monitoring of a PV-battery microgrid. The study considered the issues of limited visibility of renewable generation and battery conditions, electrical loading, voltage and frequency excursions, IoT delay, and slow detection of abnormal operating conditions in small-scaled microgrids. An IoT-enabled data acquisition system architecture was implemented to measure solar irradiance, PV voltage, current and power, load power, battery SOC, bus voltage and frequency; followed by implementation of an IoT-enabled supervisory platform for: graphical visualization of the electrical variables, generation of alarms when the measured variables were above or below their thresholds, and commands for supervisory control. Mathematical models were further derived for: PV generation, battery SOC, three-phase power, alarm activation, the effect of communication delays, supervisory control, monitoring accuracy, and system availability. The system was validated using ten samples collected from 08:00 to 12:30 hours. Results showed PV power generation increased from 2.48 kW at 08:00 hours to a maximum 7.60 kW at 11:30 hours when solar irradiance increased from 285 to 820 W/m^2. Load demand increased from 3.10 to 7.15 kW resulting in a power deficit at 08:00 hours of 0.62 kW, a power surplus of 2.05 kW at 11:30 hours, and 0.75 kW at 12:30 hours of power deficit. Battery SOC increased from 72.4 to 80.1%. Delay in communication time fluctuated between 59 to 118 ms with an average value of 74.4 ms. The bus voltage decreased to 397.4 V and frequency to 49.87 Hz at 12:30 hours before the SCADA alarm was activated. These results highlight the effectiveness of an IoT-SCADA integrated system for telemonitoring, remote supervision and control of renewables microgrids. The study guides policies for IoT communication standardization, metering calibration, minimum cybersecurity, necessary interoperability, data availability, and supervisory monitoring standard requirements for renewables microgrids.

Keywords: Internet of Things (IoT); SCADA; solar PV microgrid; battery energy storage; supervisory monitoring

1 Introduction

The rising need for a reliable, sustainable, and decentralized power supply has enhanced the installation of renewables-based microgrids especially in areas where the existing grid infrastructure is lacking, unreliable, or nonexistent. Because of its portability, reducing costs and suitability for decentralized power generation [1], solar PV generation is a preferred candidate for microgrid applications; yet, the intermittent nature of solar irradiation, changes in power demand, battery state of charge, and operating conditions pose serious difficulties in the successful operation of the microgrid. These issues are of major concern in the Bonny Island microgrid, a small, isolated community where reliable electricity supply is a vital necessity for the town's residential, commercial, industrial, and community services.

Traditional control and monitoring strategies usually involve human measurements, time-limited local meters, and scattered communicating distributed energy resources (DERs). Such systems can impede the detection of abnormal operational states and make it hard for operators to have a full picture of PV power, energy storage, load demand, voltage, current, frequency, and power flow in real time [2]. The convergence of IoT and Supervisory Control and Data Acquisition (SCADA) systems introduces solutions by establishing synergies among distributed sensors, intelligent electronic devices, communication infrastructure, and supervisory control software.

The IoT-operated SCADA system can also frequently extract the status-related values from solar PV array, battery energy-storage system, inverter, protection devices and electrical loads. These measurements can be communicated over suitable networks to a supervisor where they can be viewed, stored, interpreted, analysed and utilised to make operational choices [3]. The system can also include the features of alarm generation, record of events, remote switching, monitoring of asset-state, and analysis of historical-data, thereby allowing the operators to quickly detects anomalies in load like high/low voltage and frequency, high/low battery charge, low output of solar PV arrays and unusual patterns in load.

An IoT platform monitoring system is particularly suited for Bonny Island because the operation of a solar microgrid is reliant on the integrated operation of renewable sources, energy storage, and dynamic loads. In-situ measurements facilitate the sharing of the right energy-management information in real-time, and enhance insight into the condition of the microgrid. Additionally, past measurements can be valuable for understanding usage trends, assessing renewable energy performance, and schedule maintenance [4].

Thus, this work is oriented to construct an IoT-based SCADA system for supervisory monitoring and operational control of the solar microgrid in Bonny Island. The work takes into account the real-time gathering of electrical and environmental measurements, IoT-based communications, supervisor visualizations, alarm processing, and remote control mechanisms. The constructed SCADA system aims to enhance operational visibility, facilitate early control actions, enhance energy-management strategy, and serve as a basis for practical monitoring of reliable solar microgrid system operation.

2 Literature review

Electricity demand forecasting and renewable energy planning are vital as they help enhance energy security and promote sustainable development in Nigeria. The long-term load forecasting would assist in future estimates of electricity demand and plans for generation, transmission and distribution along with renewable-energy investments. An application of linear regression technique to Bonny and Finima revealed the practicality of using linear regression model in ensuring the demand for electricity in the near future, though this may not be practical when the demand of electricity is driven by non-linear socio-economic and environmental factors [1]. Additionally, from evidence on Nigeria's energy transition, there is still significant institutional backing on renewable-energy development and investments to replace traditional sources of energy [5].

Although all communities will benefit from renewable-energy use, coastal and environmentally-sensitive communities may find the most immediate use and greatest benefit in this sector. A review of potential pathways to sustainable development in Nigeria specifically recommended renewable-energy use as an important pathway to sustainable development, noting the potential role of clean-energy sources in providing energy security, environmental protection, and socioeconomic growth [2]. Publications exploring Nigeria's blue economy have also linked renewable-energy development

with the sustainability of the nation's maritime and coastal economies, suggesting a role for clean-energy solutions in emerging maritime industries while reducing environmental impacts [6]. This is especially true for Bonny Island, given the presence of industrial, maritime, residential, and commercial activities that generate currently significant-and potentially increasing-energy needs.

Another crucial aspect of sustainable power-generation development is power-system reliability. Phasor measurement-unit placement has been studied using an evolutionary computing algorithm for power system monitoring and to provide fault-location support in power systems [3]. Greater relay co-ordination at 11 kV distribution feeders has been evaluated, thereby highlighting the importance of adequate power protection settings for minimising the impact of electrical faults [4]. Another facet of energy planning relates to renewable-resource evaluation. An assessment of offshore wind at the Lagos site demonstrated the potential of marine wind resources [7].

Construction of infrastructure in and around Bonny, as well as in the greater Niger Delta, supports the case for more assured planning of electricity. Large transportation and maritime development projects will generate further industrial and commercial activity that in turn, will generate further demands for electricity [8]. Studies into blue-economy development reinforce the evidence for an inextricable link between economic growth and environmental protection [9]. Wave-energy screening with RETScreen has investigated potential for ocean energy development in the Bonny Island area [10].

At the distribution level, critical to the secure and reliable delivery of electricity, substation design must be adequate to meet increasing levels of transformation capacity required by growing load [11]. The forecast of future loads was identified for consideration in the planning of the extension of low-voltage power systems in rural electrification projects [12]. Power-system surge studies outlined the need for protection of electrical equipment against transient phenomena affecting the system's stability [13].

Environmental and climate dimensions are equally relevant, since climate change might impact fisheries and other economic activities of the Niger Delta and thus the projected electricity demand of the community [14]. Wind-energy site-selection analysis conducted for the community of Bonny, in the East Niger Delta, illustrates the importance of location-appropriate renewable-resource assessment for community-based sustainable energy planning [15]. In summary, the body of existing work makes transparent the relationship between load forecasting, renewable-resource assessment, network reliability, and environmental sustainability, as well as the future of economic development and planning for energy systems for Bonny Island. Yet, the literature points more to a need for consolidating studies that consider these dimensions separately and analyze demand with regard to locally available renewable-energy resources and the needs of sustainable coastal communities.

3 Methods

3.1 Development of the IoT-enabled data acquisition system

3.1.1 Solar PV power measurement

The photovoltaic measurement model calculates instantaneous solar power from measured array voltage and current. It provides the generation variable transmitted by IoT sensors, enabling real-time observation of renewable production and supporting subsequent supervisory decisions concerning storage, loading, and power balance.

$$P_{PV}(t) = V_{PV}(t)I_{PV}(t) \tag{1}$$

where $P_{PV}(t)$ is the instantaneous photovoltaic output power (W), $V_{PV}(t)$ is the measured PV array voltage (V), and $I_{PV}(t)$ is the measured PV array current (A).

3.1.2 Battery state-of-charge estimation

The battery state-of-charge model estimates stored energy from previous charge status and measured battery current over each sampling interval. It enables continuous storage monitoring, identifies charging or discharging conditions, and provides an essential variable for continuous operational supervisory energy-management decisions.

$$SOC(k) = SOC(k-1) - \frac{I_B(k)\Delta t}{Q_B} \times 100 \tag{2}$$

where SOC(k) is the battery state of charge at sample k (%), SOC(k − 1) is the previous state of charge (%), $I_B(k)$ is the battery current (A), Δt is the sampling interval (h), and Q_B is the rated battery capacity (Ah). The sign convention assumes that positive current represents battery discharge.

3.2 Design of the SCADA-based supervisory control platform

3.2.1 Three-phase active and reactive power

The three-phase power model determines active and reactive power from measured phase voltages and currents. These quantities characterize electrical loading and power flow at monitored microgrid buses, allowing the SCADA interface to display operating conditions and identify abnormal electrical states.

$$P_{3\phi}(t) = \sqrt{3}V_{LL}(t)I_L(t)\cos\phi(t),\ Q_{3\phi}(t) = \sqrt{3}V_{LL}(t)I_L(t)\sin\phi(t) \tag{3}$$

where $P_{3\varphi}$ is the three-phase active power (W), $Q_{3\varphi}$ is the three-phase reactive power (var), V_{LL} is the line-to-line RMS voltage (V), I_L is the line RMS current (A), and φ is the voltage–current phase angle.

3.2.2 SCADA alarm generation

The supervisory alarm model compares each measured operating variable with predefined permissible limits. When a variable exceeds its threshold, the system generates an alarm condition for operator visualization, event logging, and remote intervention, thereby supporting identification of abnormal microgrid operation.

$$A_x(k) = \begin{cases} 1, & x(k) < x_{\min} \text{ or } x(k) > x_{\max} \\ 0, & x_{\min} \le x(k) \le x_{\max} \end{cases} \tag{4}$$

where $A_x(k)$ is the alarm status for monitored variable x, $x(k)$ is its measured value, and x_{min} and x_{max} are the allowable lower and upper operating limits, respectively. $A_x = 1$ indicates an alarm condition, while $A_x = 0$ indicates normal operation.

3.3 Implementation of the IoT communication and control framework

3.3.1 IoT communication latency

The communication latency model quantifies elapsed time between measurement acquisition at a field device and successful reception at the SCADA server. This metric evaluates whether IoT

communication provides sufficiently timely information for monitoring, supervision, and control of distributed microgrid equipment.

$$T_{lat} = T_{rx} - T_{tx} \tag{5}$$

where T_{lat} is the communication latency (s), T_{tx} is the timestamp at which a measurement packet is transmitted by the IoT field device (s), and T_{rx} is the timestamp at which the packet is successfully received by the SCADA server (s).

3.3.2 *Supervisory control command*

The supervisory command model represents remote control decisions issued by the SCADA platform according to measured operating conditions. It defines commanded device states while incorporating communication and execution delays, thereby providing a representation of supervisory switching actions within the microgrid.

$$u(k) = f\left[P_{PV}(k),\ SOC(k),\ P_L(k),\ V(k),\ f_g(k)\right] \tag{6}$$

where $u(k)$ represents the supervisory control command at sample k; P_{PV} is PV generation; SOC is the battery state of charge; P_{L} is load power; V is the monitored voltage; and f_{g} is the grid or inverter frequency. The function $f(\cdot)$ represents the programmed SCADA control logic.

The system architecture block diagram of the four-layer IoT-enabled microgrid SCADA design is shown in Figure 1: 1) The Layer-1 shows the physical components of the architecture, which consist of PV solar array, battery bank, and the AC microgrid bus; 2) The Layer-2 showcases the IoT sensing and edge processing modules which perform the preliminary power calculations, SOC, and power quality analytics by implementing Equations 1–3; 3) The Layer-3 demonstrates data transmission with the help of IoT gateway and MQTT broker platform as well as the communication latency measurement with the help of Equation 5; and 4) The Layer-4 indicates the SCADA server engine, data historian, alarm generation logic by combining the Equation 4, supervisory control logic, and Equation 6, as well as the operator HMI (human-machine interface).

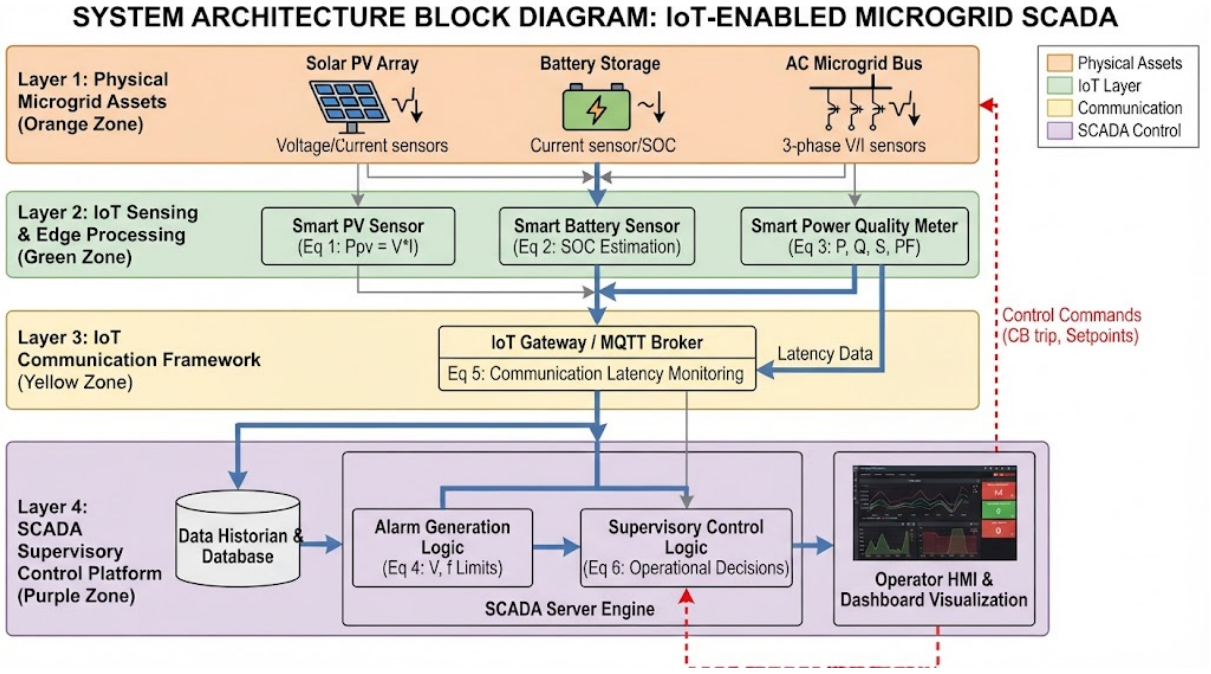


Figure 1. Architecture of the four-layer IoT-enabled microgrid SCADA system.

3.4 Evaluation of the IoT-based SCADA system

3.4.1 Monitoring accuracy

The monitoring accuracy model compares IoT-measured values with reference measurements from calibrated instruments. Mean absolute percentage error provides a normalized performance indicator for evaluating measurement quality across voltage, current, power, frequency, irradiance, and battery variables during measured experimental system operation.

$$MAPE = \frac{100}{N}\sum_{k=1}^{N}\left|\frac{x_{IoT}(k) - x_{ref}(k)}{x_{ref}(k)}\right| \tag{7}$$

where MAPE is the mean absolute percentage error (%), N is the number of observations, $x_{\mathrm{IoT}}(k)$ is the value measured by the IoT system, and $x_{\mathrm{ref}}(k)$ is the corresponding calibrated reference measurement.

3.4.2 System availability

The system availability model expresses the proportion of scheduled operating time during which the complete IoT-SCADA system remains operational and capable of monitoring or controlling the microgrid. It provides a reliability indicator for evaluating supervisory service under changing operating conditions.

$$A_{sys} = \frac{T_{up}}{T_{up} + T_{down}} \times 100 \tag{8}$$

where A_{sys} is the system availability (%), T_{up} is the total time during which the IoT-SCADA system is operational and available for monitoring or control (h), and T_{down} is the total system downtime (h). The operating data recorded by the system over the ten sampling intervals are given in Table 1.

Table 1. Measured operating data of the IoT-SCADA microgrid over the ten sampling intervals.

No.	Time	G (W/m^2)	V_{PV} (V)	I_{PV} (A)	P_{PV} (kW)	P_L (kW)	SOC (%)	V_{bus} (V)	f (Hz)	Latency (ms)	Status
1	8:00	285	318	7.8	2.48	3.1	72.4	398.2	49.96	86	Normal
2	8:30	360	325	9.6	3.12	3.35	72.1	399.1	49.98	79	Normal
3	9:00	445	331	11.7	3.87	3.62	72.6	400.3	50.01	74	Normal
4	9:30	535	338	13.9	4.7	3.88	73.5	401.2	50.02	68	Normal
5	10:00	625	344	16.1	5.54	4.2	74.8	401.8	50	65	Normal
6	10:30	710	349	18	6.28	4.65	76.4	402.5	50.03	62	Normal
7	11:00	785	352	20.2	7.11	5.1	78.2	403.1	50.01	59	Normal
8	11:30	820	355	21.4	7.6	5.55	79.7	402.7	49.99	61	Normal
9	12:00	760	351	20.1	7.06	6.2	80.1	401.9	49.95	72	Normal
10	12:30	680	346	18.5	6.4	7.15	79.4	397.4	49.87	118	Alarm (V, f)

Note: G = solar irradiance; V_{PV}, I_{PV}, P_{PV} = PV array voltage, current and power; P_L = load power; SOC = battery state of charge; V_{bus} = bus voltage; f = frequency.

4 Results and discussion

4.1 Microgrid power balance

As illustrated in Figure 2, the results show the dynamic interaction between the solar PV generation and the microgrid load power consumption, from 8:00 to 12:30. The measured photovoltaic power generation yields a daily maximum of 7.60 kW at 11:30, following the trend of solar irradiance, with initial and final PV power of 2.48 kW and 6.40 kW at 8:00 and 12:30 respectively. While the solar power drops in the afternoon, the load power consumption reaches a maximum of 7.15 kW at 12:30, showing that, while generation exceeds load in the late morning, the opposite occurs by 12:30.

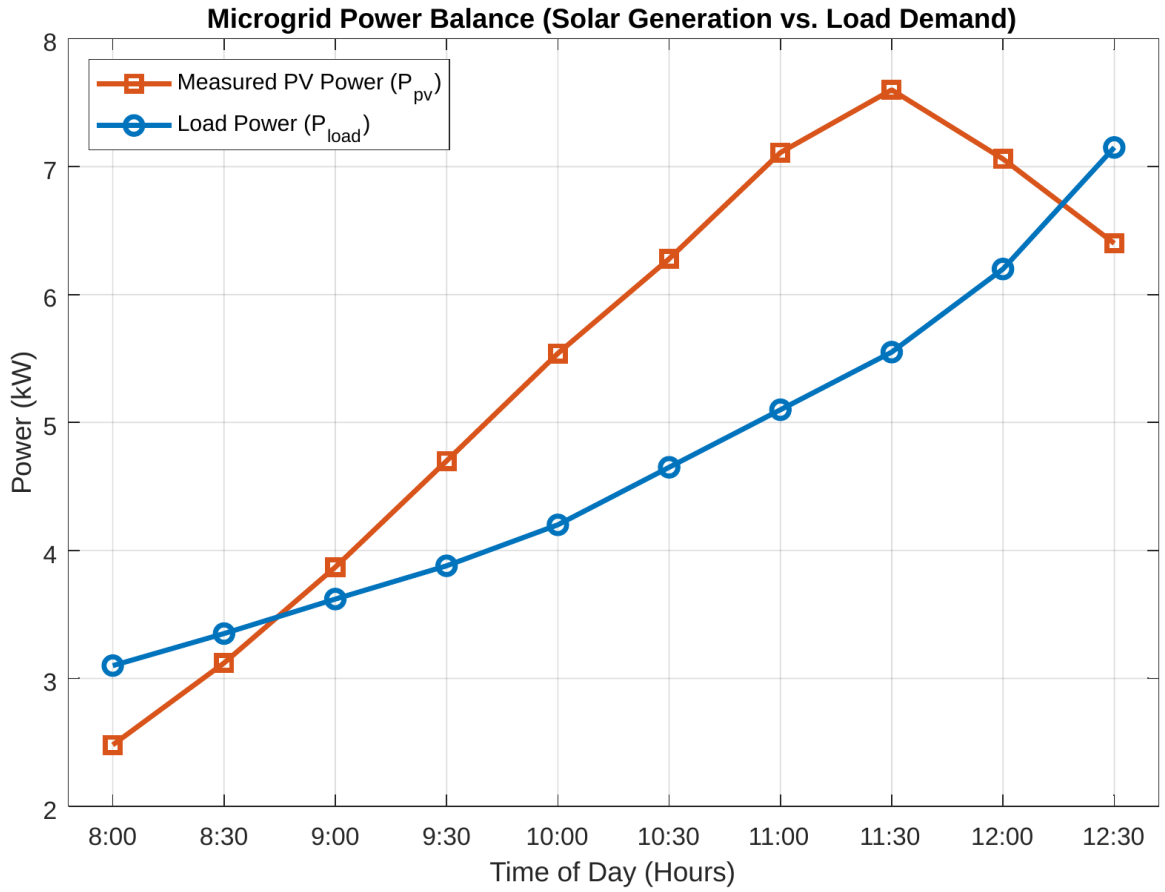


Figure 2. Microgrid power balance: PV generation versus load demand.

4.2 Battery SOC dynamics

Figure 3 graphically displays the two-axis response of the battery state-of-charge trajectory against the net microgrid power balance throughout the day. Battery state of charge (higher ordinate axis scale) begins at 72.4% at 8:00, then incrementally charges as the solar generation becomes greater than load throughout the late morning, and lastly reaches a maximum of 80.1% at 12:00 then slightly recedes again to 79.4% at 12:30 as a consequence of a net power balance of a negative system power of −0.62 kW at 8:00 up to a highest system power at 11:30 of 2.05 kW then back down to −0.75 kW at 12:30.

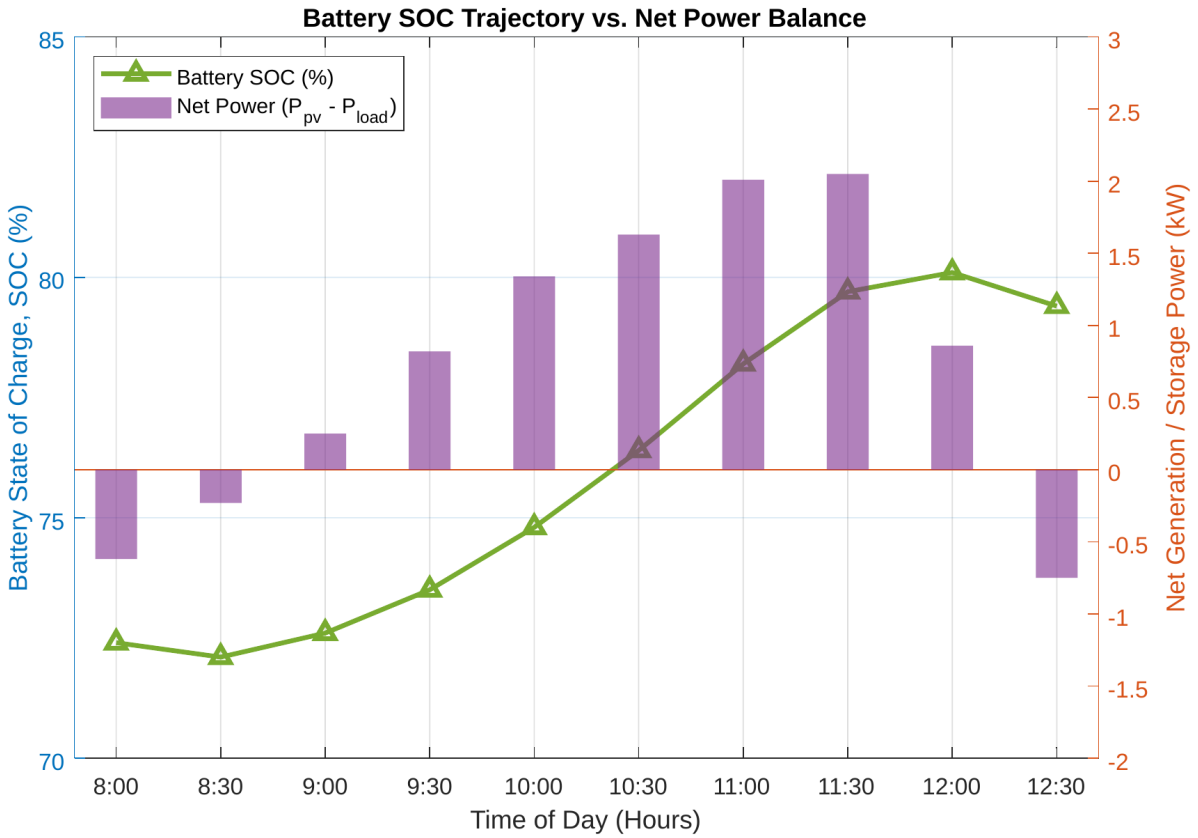


Figure 3. Battery SOC trajectory versus net power balance.

4.3 SCADA limits and alarms

The supervisor control and data acquisition limit verification shown in Figure 4 is used to check the system stability of the microgrid based on bus voltage and frequency range limit. The bus voltage is quite steady, ranging between 398.2 V at 8:00 and 403.1 V at 11:00, but it is 397.4 V at 12:30 and lower than the limit of 398.0 V. Meanwhile, the system frequency is tightly ranged between 49.96 Hz and 50.03 Hz during earlier time span, but it falls to low value of 49.87 Hz at 12:30 which is lower than the limit of 49.90 Hz and caused the SCADA alarm in real time.

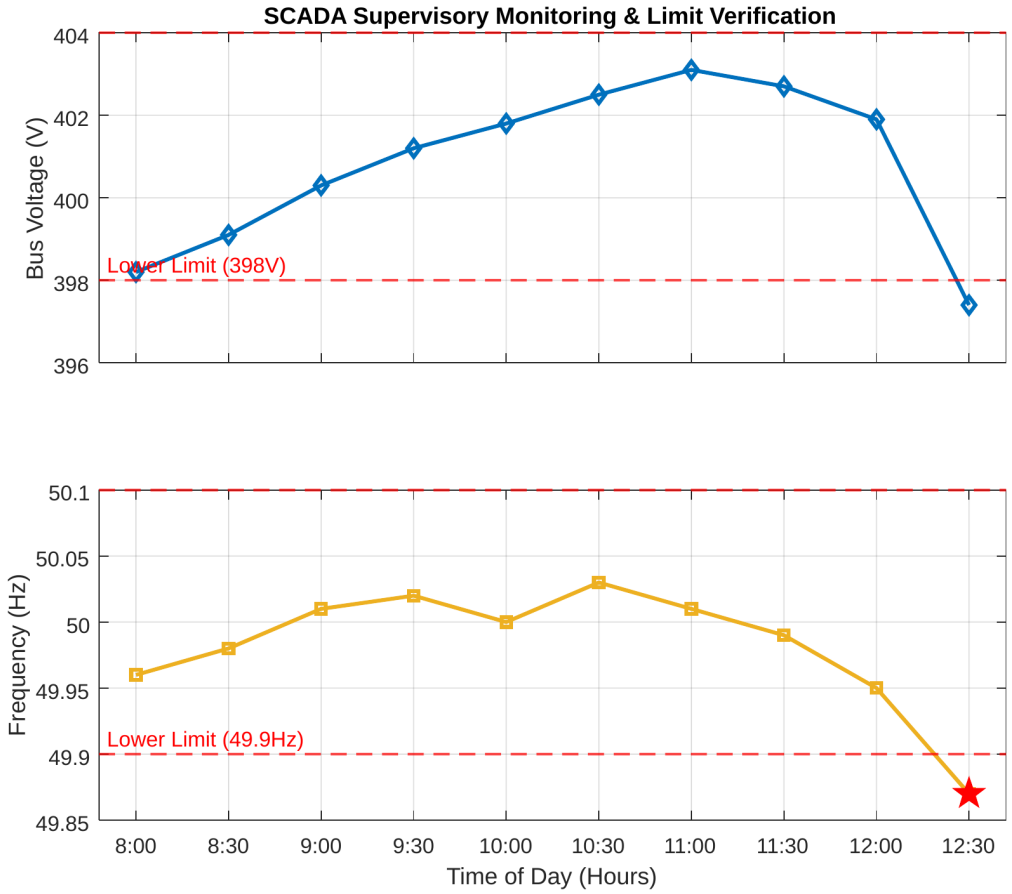


Figure 4. SCADA supervisory monitoring and limit verification of bus voltage and frequency.

4.4 IoT communication latency

Figure 5 highlights the operational performance of the IoT communication framework by plotting the elapsed latency between field sensor data acquisition and SCADA server reception. The communication latency starts at 86 ms at 8:00, progressively improves to a minimum network delay of 59 ms at 11:00 as data traffic stabilises, and eventually spikes to a peak latency of 118 ms at 12:30. Across all sampled intervals, the system maintains an average communication latency of approximately 74.4 ms, confirming that the IoT framework delivers sufficiently rapid telemetry updates for real-time microgrid monitoring.

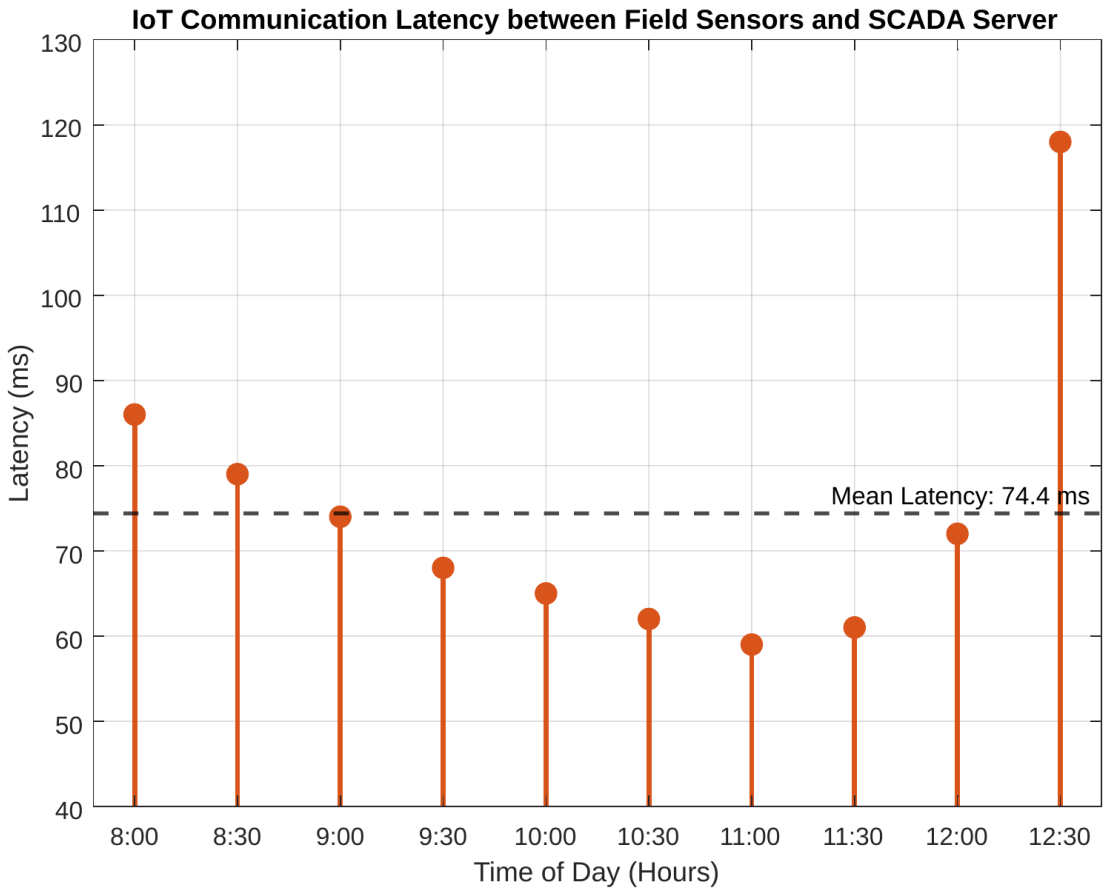


Figure 5. IoT communication latency between field sensors and the SCADA server.

4.5 Model validation

The accuracy of the mathematical photovoltaic formulation is validated in Figure 6 by comparing the calibrated field-measured PV power against the calculated analytical model output. The calculated PV power values, derived using Equation (1) as the product of measured array voltage and current divided by one thousand, closely track the actual measured values across all ten sampling intervals. For instance, at the 8:00 sampling mark the calculated power of 2.48 kW matches the measured 2.48 kW, and at the peak 11:30 interval the calculated value of 7.60 kW mirrors the telemetry measurement of 7.60 kW.

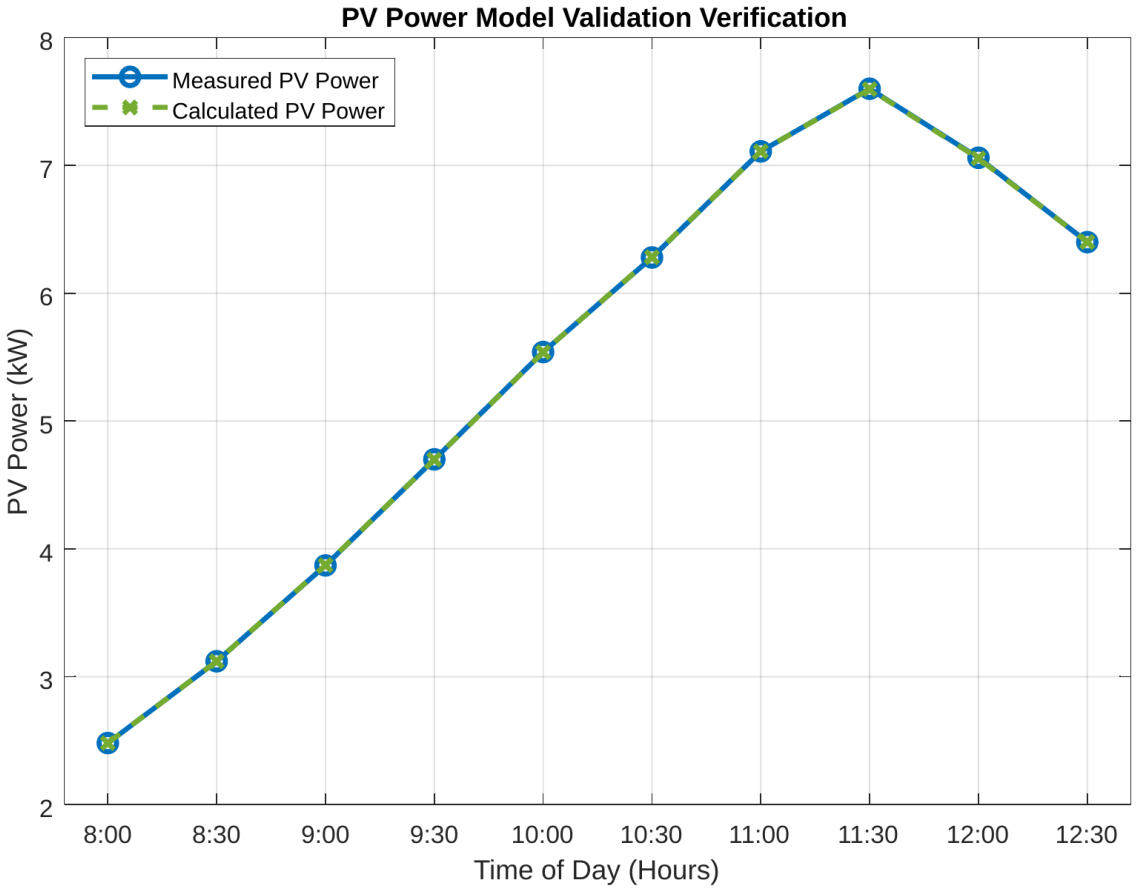


Figure 6. PV power model validation: measured versus calculated PV power.

5 Conclusion

This paper successfully designed, implemented and tested a real-time IoT-based SCADA platform for solar microgrid supervision and real-time control. The combined SCADA used PV generation, battery state-of-charge, electrical load, bus voltage and frequency, communication latency and alarm readings as input data streams from a non-isolated distributed sensor set on the microgrid. Results showed that the IoT-enabled SCADA was able to provide static visualization of key electrical variables and dynamic identification of changing generation, storage and load states.

Developed PV, battery and power-monitoring models demonstrated that the system was able to provide continuous feedback of operations and therefore meaningful identification of changes in generation and load.

The developed PV power-model was able to replicate the instantaneous PV power generation from the measured array voltages and currents. Of 10 sample points, the PV array power generation started at 2.48 kW at 8:00, reached a maximum value of 7.60 kW at 11:30 and then reduced to 6.40 kW at 12:30 as the PV array output decreased in conjunction with reductions in array irradiance from 285 to 820 W/m^2 and its subsequent decline to 680 W/m^2. The very close agreement between calculated and measured values of PV power demonstrates the ability of the power model to accurately mimic real-time PV output for use in operator supervision and energy management. The battery state-of-charge results demonstrated that the use of real-time battery state-of-charge measurement offered useful supervision and management information.

Estimated state-of-charge starting from 72.4% at 8:00, increased to 80.1% by 12:00 and then dropped to 79.4% at 12:30 as PV power generation became available and demand through the bus line exceeded generation.

Accurate ongoing monitoring of battery and, consequently, load status, has potential to inform routine energy management decisions. The SCADA platform enabled visual-standalone time-series monitoring of bus voltage and frequency over the ten sample periods. Unusually high equipment load was reflected in a drop in bus voltage to 397.4 V and the recorded abnormal alarm at 12:30, when bus voltage dropped to this value and frequency dropped to 49.87 Hz. This confirmed the alarm functionality of the IoT-SCADA supervisory platform. The IoT communication assessment showed that data recording accuracy was maintained by the IoT devices over the evaluation period with the lowest communication latency at 59 ms on 11:00. Latency increased at 12:30 to 118 ms, demonstrating that communications latency can vary with operating conditions and access network efficiency, highlighting the importance of ongoing communication monitoring in IoT applications.

Overall, the developed IoT-SCADA architecture was able to undertake combined measuring and communicating tasks, coupled with visualization and alarm generation, to greatly improve the state-of-the-art in solar microgrid supervision.

Developed combinations of real-time PV power, battery state-of-charge, electrical-variable, alarm and communication-latency measurement tools offer a valuable platform of practical generalizability for supervision in small distributed renewable energy systems. Future work can extend this work through use of larger sampling datasets, field trials, implementation of control algorithms, power system safety mechanisms, cyber-security features and fleet forecasting functions.

References

[1] Adebayo AD, Emu C. *Long-term electric load forecasting for Bonny and Finima towns using linear regression method*. International Journal of Engineering Research and Technology (IJERT). 2019;8(11). https://doi.org/10.17577/IJERTV8IS110248

[2] Amadi HN, Bakare BI, Igbogidi ON. Renewable energy for sustainable development in Nigeria: A comprehensive review. In: *Proc*. 1st Int. Conf. Faculty Environmental Sciences, Nnamdi Azikiwe University. 2024. p. 116–135.

[3] Amadi HN, Maxwell WS, Ijeoma RC. Evolutionary computing heuristics of the optimal phasor measurement units placement for fault location in power system networks. *European Journal of Advances in Engineering and Technology (EJAET)*. 2025;12(2):1–9.

[4] Amadi HN, Okosi F, Ijeoma RC. Simulation and analysis of improved relay coordination in Tungbo 11 kV feeders in Sagbama Substation, Bayelsa State, Nigeria. *European Journal of Advances in Engineering and Technology (EJAET)*. 2024;11(11):41–49.

[5] African Development Bank (AfDB) . *African Development Bank (AfDB) commits $1.2 million grant to support Nigeria's energy transition*. ESI-Africa. 2025.

[6] Amadi HN, Biragbara P, Horsfall DJ, Dike B. Advancing Nigeria's blue economy: The role of renewable energy in sustainable coastal and marine economic growth. In: *Proc*. Int. Conf. Faculty Engineering (ICOFE), Niger Delta University. 2024. p. 1–15.

[7] Attah A, Abubakar JA, Badejo J. Assessing the technical offshore wind energy potential in Lagos, Nigeria. *IOP Conference Series: Earth and Environmental Science*. 2021;730(1):012036. https://doi.org/10.1088/1755-1315/730/1/012036

[8] BusinessDay . *Nigeria leaps into AfCFTA with $3.2bn Eastern rail project, Bonny Deep Seaport*. 2025. 2025.

[9] Dike SC. *Nigeria's blue economy: Economic and environmental sustainability*. ResearchGate. 2025.

[10] Emu C. *RETScreen-based techno-economic study of wave energy potential in Bonny Island, Nigeria*. Journal of Energy Research and Reviews. 2025.

[11] Ijeoma RC, Olisa IE. Design of 3-phase, 50 Hz, 500 kVA, 33/0.4 kV distribution substation. *IOSR Journal of Electrical and Electronics Engineering (IOSR-JEEE)*. 2019;14(4):38–48.

[12] Ijeoma RC, Odu EV. Future load energy forecast of Stone-City, Mgbede Community rural electrification scheme. *International Journal of Science, Engineering and Technology (IJSET)*. 2025;13(3):1–9.

[13] Ijeoma RC, Odu EV. Power system surges: Causes, effects, and mitigation strategies. *International Journal of Science, Engineering and Technology (IJSET)*. 2025;13(3):10–17.

[14] Ikehi ME, Zimoghen J. *Impacts of climate change on fishing and fish farming in the Niger Delta region of Nigeria*. ResearchGate. 2025.

[15] Jackson KP, Hart L, Benjamin BE, Brown I. Site selection for wind energy as an alternative source of energy in Bonny, Nigeria. *Asian Journal of Geographical Research*. 2024;7(1):71–86. https://doi.org/10.9734/AJGR/2024/v7i1207

[16] Energy Digital. *Digital Energy Challenge for Start: Call for projects* [Internet]. 2025.